

Short Communication

## **Durability and Degradation of Concrete Obtained from Binary Mixtures of Fly Ash and Steel Slag Activated Alkali**

W. Aperador<sup>1,\*</sup>, E. Ruiz<sup>1</sup>, J. Bautista-Ruiz<sup>2</sup>

<sup>1</sup> School of Engineering, Universidad Militar Nueva Granada, Bogotá-Colombia

<sup>2</sup> Universidad Francisco de Paula Santander, San José de Cúcuta, Colombia

\*E-mail: [g.ing.materiales@gmail.com](mailto:g.ing.materiales@gmail.com)

Received: 30 June 2015 / Accepted: 27 July 2015 / Published: 30 September 2015

---

In order to meet the mechanical requirements, design and cost, in the field of civil engineering and producing a lesser impact to the environment in its production of concrete mixtures of steel blast furnace slag and fly ash from power plants they were obtained activated carbon using sodium silicate ( $\text{Na}_2\text{SiO}_3$ ) at a concentration of 5%  $\text{Na}_2\text{O}$ . Were evaluated performance durability of concrete by penetration tests chloride ion and compressive strength at 28 days, degradation evaluated corresponds to steel embedded in the ceramic matrix, which was done using techniques measurement of OCP (corrosion potential) and Tafel polarization curves for this track under conditions simulating seawater (3.5% saline is performed for NaCl). We was found that significantly decreased the corrosion rate of the steel samples with higher content of fly ash, the opposite effect reported for the mechanical strength, confirming the good performance of binary mixtures.

---

**Keywords:** fly ash, steel slag, mechanical strength, corrosion, chloride ion.

### **1. INTRODUCTION**

The coal used in the power plant is crushed, pulverized and later introduced into the combustion chamber. The organic components are oxidized and volatilized during combustion while a large part of the mineral matter is transformed into solid waste by products: fly ash and slag [1-3]. Fly ash is composed of particles you because of its small size are entrained by the flow of gas generated during coal combustion. Fly ash to retain gas flow leaving the combustion chamber and prevent them from being emitted into the atmosphere is used; a retention system called electrostatic precipitator, which exhibits greater efficiency, usually higher than 99.5% [4-5]. Fly ash is collected in the hoppers

of the electrostatic precipitators, from where they are transported to storage sites, often located in settling basins or dry.

Fly ash generally exhibit an outer covering on a reactive glass matrix mainly composed of Si-Al. This layer enriched in most of the elements of environmental interest, such as As, Cr, Cs, Mo, S, Sb, Se, V and Zn, due to condensation processes [6-7].

The by-products of coal combustion in power plants obtained are usually composed of more than 70% of aluminosilicate glass material [8]. This composition allows their utilization in civil engineering alternatively in mine filled and alternative source in the extraction of Al, Fe, Si, Ge, Ga, V and Ni, and soil additives [9-11].

The granulated blast-furnace slag has been used successfully as a partial or total substitute for ordinary Portland cement in concrete mixtures, which allows obtaining materials with improved mechanical performance and durability [12-15]. Furthermore, it contributes to sustainable development through the reduction in CO<sub>2</sub> emissions and lower consumption of natural resources.

Exposure of alkali activated slag concrete against marine environments generates chlorides diffuse into the concrete, steel and can reach, according to the concentration to rupture of the passive layer protecting the steel, causing oxidation, and this leads to the decrease in the mechanical strength [16-18]. Reinforcing steel embedded in concrete is protected from corrosion due to the high alkalinity of the medium, specifically steel-matrix interface. However, this protection status may be terminated by the destruction of the passive film due to the ingress of aggressive ions (such as chloride or sulphate) or by reducing, the pH in the area covered by the armature (carbonation) and thus loss of mechanical properties and decreased life [19]. However, detailed studies of the electrochemical behaviour of reinforcing steel they indicate that has a susceptibility to degradation. Therefore, the need to evaluate the interaction of reinforcement materials and industrial by-products are undergoing especially under aggressive conditions is seen as worldwide deterioration of structures due to the corrosion is a problem that leads to high costs of maintenance and / or repair [20-21].

Various electrochemical methods reported in the literature, such as measurement of OCP (corrosion potential,  $E_{corr}$ ), linear polarization resistance (LPR) and Tafel polarization curves, to assess the behaviour of steel embedded in concrete structures [22-25]. These methods and  $E_{corr}$  contrast to stationary LPR techniques (anodic polarization), permits the characterization of a non-destructive manner on diffusion of aggressive species into the concrete and the kinetics of the electrochemical reactions that occur on the steel surface [26]. The steel-reinforced concrete is the construction material used for the production of structures; however, the integrity of the reinforcements affected when the concrete is put under severe conditions where the durability of the material is reduced by phenomena such as corrosion, by chloride ion [27].

This article presents the results obtained on the properties of durability and degradation of concrete mixtures obtained with the corresponding industrial products to steel slag and ash wheel when subjected under marine conditions. Were performed measurements of OCP (corrosion potential,  $E_{corr}$ ) and Tafel polarization curves at different exposure times. The values generated they were compared with penetration tests chloride ion and compressive strength, in order to find a correlation.

## 2. EXPERIMENTAL DETAILS

### 2.1. Materials

This study has used Class F fly ash and granulated blast furnace slag. Tables 1 and 2 register the physical and chemical properties of cementations materials.

**Table 1.** Physical properties of cementations materials used.

	Specific weight, g/cm <sup>3</sup>	Specific surface, m <sup>2</sup> /g	% unburned
Steel slag	3.0	2.7	----
Fly ash	2.6	3.6	12%

**Table 2.** Chemical composition of the fly ashes, the steel blast furnace slag.

Compound	Fly ash (in mass %)	Steel slag (in mass %)
SiO <sub>2</sub>	54.3	33.7
Al <sub>2</sub> O <sub>3</sub>	22.8	12.8
Fe <sub>2</sub> O <sub>3</sub>	5.8	0.48
CaO	6.9	45.4
MgO	0.8	1
Na <sub>2</sub> O	0.9	0.12
K <sub>2</sub> O	1.7	1.5
P <sub>2</sub> O <sub>5</sub>	0.7	
TiO <sub>2</sub>	1.6	0.5
MnO	0.01	-
SO <sub>3</sub>	0.92	-
SiO <sub>2</sub> /Al <sub>2</sub> O <sub>3</sub>	3.5	2.63

The used aggregates correspond to a gravel with 19 mm maximum size, 2940 kg/m<sup>3</sup> specific gravity, 1860 kg/m<sup>3</sup> compact unitary mass, 1700 kg /m<sup>3</sup> loose unitary mass, and 1.3% absorption. A sand with 2470 kg/m<sup>3</sup> specific surface area, 1670 kg/m<sup>3</sup> compact unitary mass, 1580 kg /m<sup>3</sup> loose unitary mass, and 2.9% absorption. Tables 3 and 4 presented the granulometry of aggregates used.

**Table 3.** Granulometry of the sand and gravel.

No S ieve	GRAVEL					SAND			
	Abertura sieve (mm)	Weight retained (g)	% retained	% accumulated retained	% pasa acumu	Weight retained (g)	% retained	% accumulated retained	% pasa acumu
1”	25.4	0	0	0	100				100
3/4”	19	37.3	1.86	1.86	98.14				100
1/2”	12.7	400.6	20	21.86	78.14				100
3/8”	9.51	718.2	35.85	57.71	42.29	0	0	0	100
4	4.76	795	39.68	97.39	2.61	27	2.85	2.85	97.15
8	2.38	52.3	2.61	100	0	32.6	3.44	6.29	98.71
16	1.19			100		49.7	5.25	11.54	88.46
30	0.6			100		147.3	15.56	27.1	72.9
50	0.3			100		433.6	45.80	72.9	27.1
100	0.15			100		256.6	27.10	100	0

**Table 4.** Properties associated with sand and gravel.

	Gravel	Sand
Absorption capacity %	0.81	5.80
Surface moisture %	0.37%	16.26
Moisture %	0.40%	1.05
Fineness modulus	6.57	2.21
Maximum size	1”	
TMN	¾”	
Bulk density [g/ml]	3.00	2.64

2.2. Concrete mixtures

The mixtures was designed to cementations material content of 448 kg / m<sup>3</sup> and a solid / liquid ratio of 0.45. For such purposes, the binary mixtures were combining different cementations materials. Thus, mixtures of fly ash with partial replacements of blast furnace slag in geopolymer concrete mixtures solely by interaction of the fly ash and slag were prepared. Table 5 summarized the proportions of the blends. The nomenclature used in the identification of mixtures is as follows: F and S identify wheel and ash materials blast furnace slag, respectively. Were also introduced to the nomenclature replacement percentages main cementations material for example, F10-S0 represents the mixture of 100% fly ash and 0% blast furnace slag; F8-S2 represents the mixture of 80% fly ash and 20% blast furnace slag.

**Table 5.** Mixture compositions.

Sample	Binder material
F0S10	100% granulated blast-furnace slag
F10S0	100% fly ash
F2S8	20% fly ash and 80% slag
F4S6	40% fly ash and 60% slag
F6S4	60% fly ash and 40% slag
F8S2	80% fly ash and 20% slag

### 2.3. Fly Ash - Steel slag

Binary mixtures of fly ash, blast furnace slag were activated by sodium silicate ( $\text{Na}_2\text{SiO}_3$ ) at a concentration of 5%  $\text{Na}_2\text{O}$ . As a cementations material it was used and additions of fly ash, blast furnace slag in different percentages. In the casting process, aggregate and cementations materials were dry blended with the help of a mixer spin for five minutes, then on the dry materials enough activator and the liquid plasticizer was added, and the mixing process continued for five minutes. Each mixture fresh, was poured into molds and compacted properly by traditional methods. The mixtures with different contents of fly ash were cured under a regime of 85 °C for 24 hours and later his specimens were demolded and housed in a storage room with room temperature until the day of test. Particularly, the specimens of the mixture with 100% slag (S10 F0) were demolded and it stored under humid conditions (90% RH) until test day.

### 2.4. Tests performed

The compressive strength of the concrete samples after 28 days of curing was evaluated; an automated system that controls a hydraulic press with 2000 kN capacity, which was used for compression tests was used.

For determining chloride ion permeability of concrete ASTM C1202 standard, it were used measuring the passage of electric current there through. The measurements was made at 28-day cure using an equipment PROOVE'it Germann Instruments.

Steel rebar corrosion over time were monitored using two techniques: (i) Corrosion potential ( $E_{\text{corr}}$ ) values. The  $E_{\text{corr}}$  parameter, may be used to define the corrosion probability:  $E_{\text{corr}} < -0.35$  V vs. Cu/CuSO<sub>4</sub> high corrosion probability (~90%),  $-0.35$  V  $< E_{\text{corr}} < -0.20$  V vs. Cu/CuSO<sub>4</sub> uncertainty of corrosion, and  $E_{\text{corr}} > -0.20$  V vs. Cu/CuSO<sub>4</sub> a 10% corrosion probability; (ii) curves polarization. The curves were obtained at 1.0 mV/s sweep rate in  $-0.3$  V<sub>SCE</sub> to 0.3 V<sub>SCE</sub> range. The corrosion level may be defined according to the Durar Network Specification [16]:  $i_{\text{corr}} < 0.1$   $\mu\text{A cm}^{-2}$  passivity,  $0.1$   $\mu\text{A cm}^{-2} < i_{\text{corr}} < 0.5$   $\mu\text{A cm}^{-2}$  low corrosion,  $0.5$   $\mu\text{A cm}^{-2} < i_{\text{corr}} < 1.0$   $\mu\text{A cm}^{-2}$  high corrosion, and  $i_{\text{corr}} > 1.0$   $\mu\text{A cm}^{-2}$  very high corrosion. Measurements were performed by Gamry 3000 electrochemical equipment at room temperature, using a cell composed of the working electrode with 1 cm<sup>2</sup> exposed area, saturated calomel electrode as reference electrode and a platinum wire as counter electrode; chloride ion as

solution. Due to the purpose of the study was to analyze the effect of chloride ions on the corrosion of reinforcing steel. The specimens were immersed in 3.5% sodium chloride saturated by 21 weeks.

### 3. RESULTS AND DISCUSSION

#### 3.1 Chloride ion penetration

The values of total charge transferred (Coulombs) in the concrete under study; calculated from the method of ASTM C1202 standard; They are presented in Figure 1, in the case of alkali activated concrete mixes has been identified that the pore solution has a very high ionic content (especially Na<sup>+</sup>). The Na<sup>+</sup> ions present in the pores of the material could try to diffuse through the sample opposite to the diffusion of Cl<sup>-</sup> ion address, which consequently cause an increase in the total charge transferred without movement taking place additional the Cl<sup>-</sup> [28-29].

The concrete mixtures showed transferred charges; in the range between 1000 and 2000 Coulombs, which classifies them as materials with low chloride permeability [30]. In concrete made only of steel slag an increase above 2000 Coulomb appreciated, therefore the system is more chloride permeability value. Which would be consistent with the diffusion of Na<sup>+</sup> ions through the sample to increase the alkalinity of the pore solution [31-32]. The addition of 20% fly ash in the cementations it generates a reduction of 5% in permeability ion chloride of concrete, being more noticeable for mixing in wherein substitution is 40% fly ash where declines is 18%.

As can be concluded in particular in the studio where the percentage of fly ash increases leads to a reduction in load last therefore, there is a decrease in the chloride permeability.

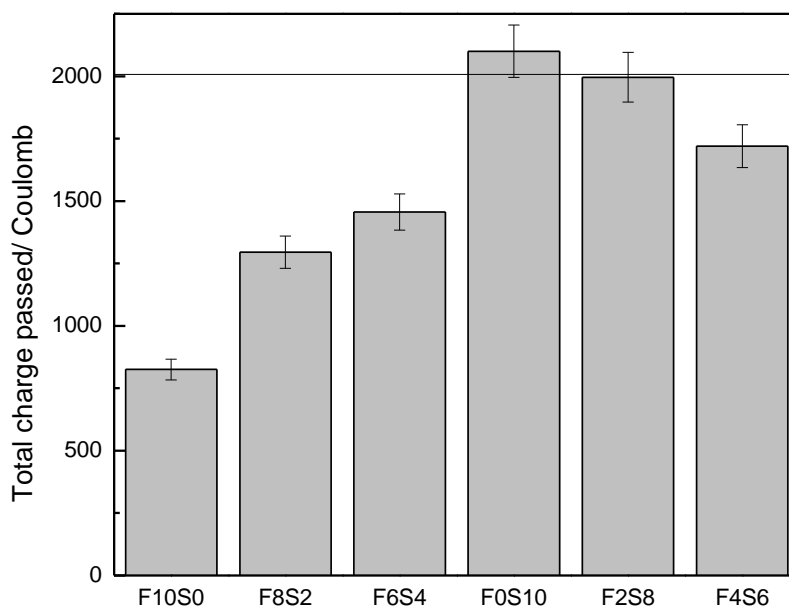


**Figure 1.** Ionic charge of alternative cements and binary mixtures.

### 3.2 Half-cell potential

In Figure 2, is exposed the measurement of OCP of concrete for each exposure age. In the case of concrete with 100% fly ash, these values were in the range of -232 mV vs -215mv and SCE, throughout the completion of the test, tending to protection values, we find that the system is under anodic control [16]. The results found are found consistent with those reported by other researchers, where alkali activated materials they have potential lower than those -300mV [16] [19]. The response of steel is observed in mixtures of 7 weeks after induction remains passive unstable film. This is oscillation in samples with some percentage of steel slag with lower values of potential with respect to the reduction of the concentration of fly ash, passive film remains more stable without steel slag, corresponding to this is found in the chloride ion penetration, because the fly ash concretes with generate less transmission chloride ions by ratifying in a way that products seal the pores in the samples with fly ash, reducing corrosion processes [33-34].

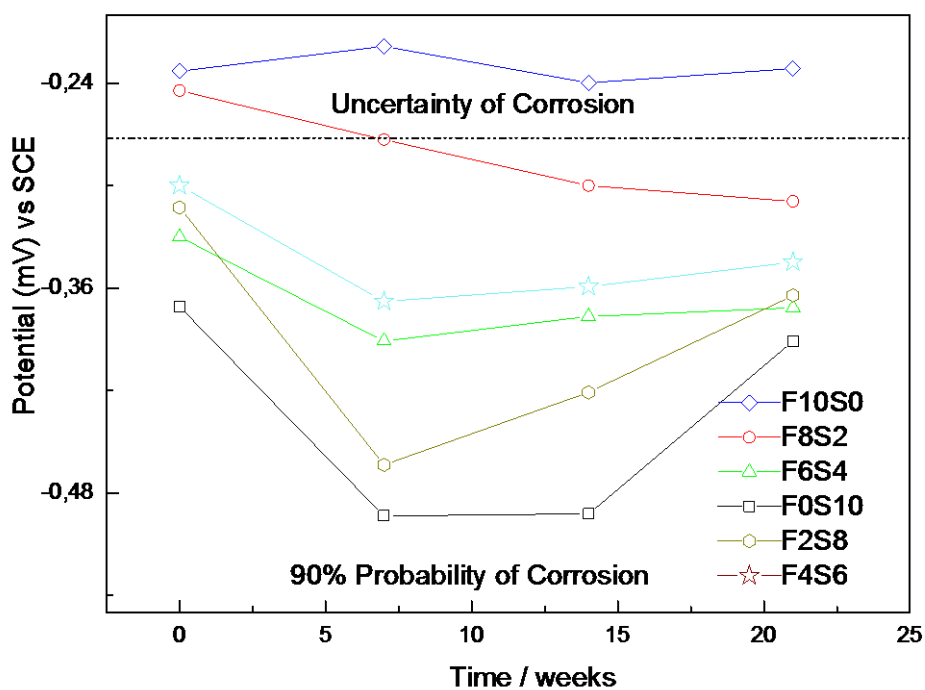


**Figure 2.** Half-cell potential values versus time for steel rebars embedded in mixtures of fly ash and steel slag. Evaluation by 21 weeks.

### 3.3 Polarization curves

In this electrochemical technique corrosion, the current is obtained by extrapolation of the cathodic and anodic regions in the measurement of OCP [35]. Furthermore, it is possible to calculate Tafel slopes, which are useful kinetic parameters to calculate the corrosion rate. The main disadvantage of the Tafel extrapolation, is the alteration of the interface of stable thermodynamic conditions, with the possibility that not to restored the initial steady state, or take long time, due

thermodynamically irreversible process. Thus, the system never returns into its initial state or steady state, so these tests are then performed of the 21 weeks, primarily because of its destructive nature.

In Figure 3, the Tafel curves for the concretes tested in 3.5% NaCl solution a fluctuation measurement of OCP is presented, with a tendency to more cathodic respect to  $E_{corr}$  values as the amount of steel slag in the mixture is increased in turn is observed remarkable increase in corrosion rate, this growth is exponential [36]. By contrast, in the absence of steel slag it shifts the potential in the anodic direction and decreases the corrosion current. Therefore, we can inferred a degradation process due to the generation of a greater shift towards corrosion density low values concretes obtained in 100% steel slag, creating a contrast in these two situations studied.

With respect to mixtures having a high component steel slag, they generate a shift towards more negative potential generating a measure of active corrosion. Corrosion density of F8S2 system it shows a large increase compared to that found in concrete F10S0; then the following combinations ramping up this Tafel slopes is observed between -0.34 and -0.095 V vs  $E_{corr}$ ; because that in each evaluation level is higher the amount of chlorine ion; that has reached the surface of the steel. The type of curves found in each of the cases they studied including F10S0 indicates a type of general corrosion by the shape of the curve shown in all cases studied.

Correlating these results with the test for resistance to penetration of chloride ion, the results are intrinsically related with moisture content of the concrete. Since rapid testing of chloride ion permeability it is essentially a measure of electrical conductivity which it depends on the pore structure and chemistry of the solution thereof for a given specimen size and applied voltage, the initial current recorded can be taken as representative of the electrical conductivity of the sample. The concrete steel slag have a higher electrical conductivity than the fly ash concrete; it indicated that the chemistry of the pore solution appears to contribute more to the electrical conductivity or charge passed to the pore structure [37].

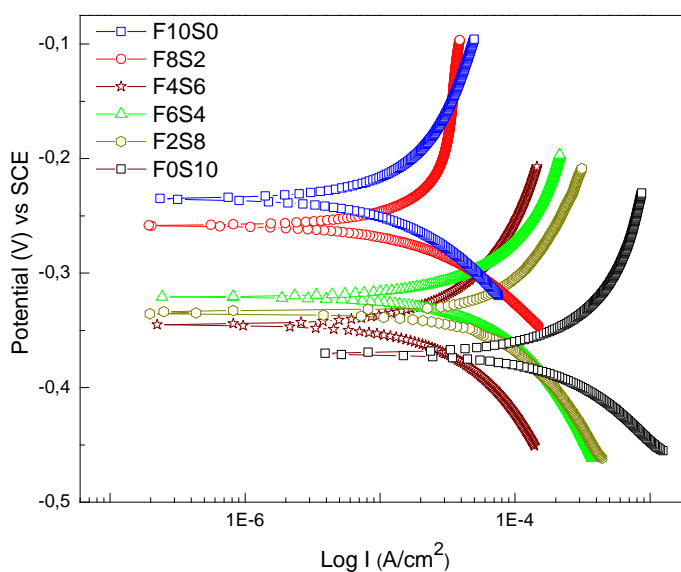


**Figure 3.** Polarization curves where it represents the electrochemical behaviour of concrete evaluated.

3.4 Compressive strength

As shown in Figure 4, the compressive strength of concrete at 28 days of curing the best performance is obtained in systems that contain higher percentage of steel slag. These being influenced by a number of factors such as the specific composition, the characteristics of the activator and the curing conditions values. Regarding the alkaline activator has been identified that this is the main factor affecting the mechanical performance of cementations with activated slag additions, It is reported the highest mechanical resistance when the cementing is based solely on steel slag [17]. In the case of activated mixtures brings a significant shrinkage of the material; leading to reductions in mechanical strength at early ages curing. The negative effect in terms of mechanical strength with the addition of fly ash, can possibly identify these driving conditions are not optimal for promoting the reaction in the fly ash [19, 38]. The improvement of the final performance of the concrete produced from these materials (fly ash and steel slag). It is also affected by the degree of thermal activation of the clay mineral, initially it depends on the amount and type of clay content in raw materials and process conditions geopolymerization such as the molar ratios of the oxides composing the system ( $\text{SiO}_2 / \text{Al}_2\text{O}_3$  and  $\text{M}_2\text{O} / \text{SiO}_2$  being the alkali ion M incorporated into the system) [22, 39]. It may indicate with a higher ratio of  $\text{SiO}_2 / \text{Al}_2\text{O}_3$  (Table 2), produces a decrease in mechanical strength.

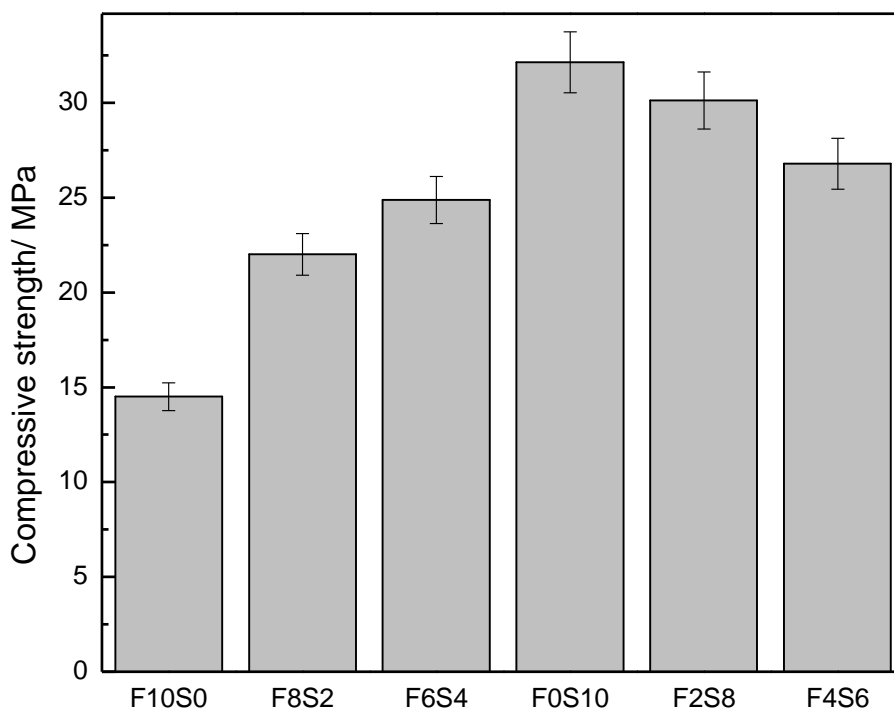


**Figure 4.** Compressive strength alternative concrete based on fly ash and steel slag and evaluated at 28 days.

#### 4. CONCLUSIONS

We found that the addition of fly ash in cementitious systems contributes to the substantial reduction of the chloride ion penetration. Steel embedded in concrete fly ash are in passive state and active state for concrete with steel slag. The corrosion current values ( $I_{corr}$ ) were obtained higher for specimens with high content of steel slag these trends are consistent with those observed in trials of Half-cell potential and polarization curves Tafel. The mechanical strength of the concrete alkali activation shows better performance in those obtained from mixtures of steel slag produced equal and design. This material can be considered high performance. However, it should be noted its high susceptibility to the lack of reaction of fly ash activator generating a decrease in mechanical strength.

#### ACKNOWLEDGEMENTS

This research was supported by "Vicerrectoría de investigaciones de la Universidad Militar Nueva Granada" under contract ING 1572.

#### References

1. P. K. Sarker, S. Mcbeath, *Constr. Build. Mater.* 90 (2015) 91
2. A. Castel, S. J. Foster, *Cem. Concr. Res.* 72 (2015) 48
3. P. K. Sarker, S. Kelly, Z. Yao, *Mater. Des.* 63 (2014) 584
4. U.A. Shaikh, W.M. Supit, *Constr. Build. Mater.* 82 (2015) 192
5. A. M. Rashad, *J. Cleaner Prod.* 93 (2015) 47
6. M. Talha Junaid, Obada Kayali, Amar Khennane, Jarvis Black, *Constr. Build. Mater.* 79 (2015) 301
7. S. Yoon, P.J.M. Monteiro, D. E. Macphee, F. P. Glasser, M.S. Eldin, *Constr. Build. Mater.* 54 (2014) 432
8. P. Gomathi, A. Sivakumar, *Constr. Build. Mater.* 77 (2015) 276
9. Z. Yu, G. Ye, *Constr. Build. Mater.* 48 (2013) 764
10. M. Arezoumandi, J. S. Volz, *J. Cleaner Prod.* 59 (2013) 120
11. P. Nath, P. K. Sarker, *Cem. Concr. Compos.* 55 (2015) 205
12. Djamel Beggas, Jahid Zeghiche, *Sustainable Cities and Society*, 6 (2013) 22
13. V. Ducman, A. Mladenović, The potential use of steel slag in refractory concrete, *Mater. Charact.* 62 (2011) 716
14. Marco Pasetto, Nicola Baldo, *J. Hazard. Mater.* 181 (2010) 938
15. M. Maslehuddin, A.A. Naqvi, M. Ibrahim, Z. Kalakada, *Ann Nucl Energy.* 53 (2013) 192
16. W. Aperador, R. Mejía de Gutiérrez, D.M. Bastidas, *Corros. Sci* 51 (2009) 2027
17. Perviz Ahmedzade, Burak Sengoz, *J. Hazard. Mater.* 165 (2009) 300
18. İ. B. Topçu, A. R. Boğa, *Mater. Des.* 31 (2010) 3358
19. M Maslehuddin, Alfarabi M Sharif, M Shameem, M Ibrahim, M.S Barry, *Constr. Build. Mater.* 17 (2003) 105
20. H.W. Song, V. Saraswathy, *J. Hazard. Mater.* 138 (2006) 226
21. D.G. Montgomery, G. Wang, *Cem. Concr. Res.* 22 (1992) 755
22. L. Bertolini, F. Bolzoni, M. Gastaldi, T. Pastore, P. Pedferri, E. Redaelli, *Electrochim. Acta.* 54 (2009) 1452
23. S. Sajedi, Q. Huang, *Eng. Struct.* 99 (2015) 120
24. H. Zhou, J. Lu, X. Xv, B. Dong, F. Xing, *Constr. Build. Mater.* 93 (2015) 257
25. A. Legat, *Electrochim. Acta.* 52 (2007) 7590

26. C. Y. Kim, J. K. Kim, *Constr. Build. Mater.* 22 (2008) 1129
27. T.T.H. Nguyen, B. Bary, T. de Larrard, *Cem. Concr. Res.* 74 (2015) 95
28. S. Kandasamy, M. H. Shehata, *Constr. Build. Mater.* 53 (2014) 267
29. W. T. Kuo, C. C. Liu, J. Y. Wang, *Constr. Build. Mater.* 49 (2013) 40
30. I. Ismail, S. A. Bernal, J. L. Provis, R. S. Nicolas, D. G. Brice, A. R. Kilcullen, S. Hamdan, J.S.J. van Deventer, *Constr. Build. Mater.* 48 (2013) 1187
31. W. Wongkeo, P. Thongsanitgarn, A. Ngamjarurojana, A. Chaipanich, *Mater. Des.* 64 (2014) 261
32. Q. Wang, J. Yang, P. Yan, *Powder Technol.* 245 (2013) 35
33. A. Fuller, M. Carbo, P. Savat, J. Kalivodova, J. Maier, G. Scheffknecht, *Renewable Energy.* 75 (2015) 899
34. M. Berra, T. Mangialardi, A. E. Paolini, *Constr. Build. Mater.* 76 (2015) 286
35. M.L. Berndt, *Constr. Build. Mater.* 23 (2009) 2606
36. G. Li, N. Otsuki, Y.S Yuan, *Procedia Earth Planet. Sci.* 1 (2009) 742
37. G. S. Brzozowska, H. Díaz, J. Maier, G. Scheffknecht, *Energy Procedia.* 37 (2013) 1462
38. G. Roa-Rodríguez, W. Aperador, A. Delgado, *Int J. Electrochem Sci.* 8 (2013) 5022
39. J. Román, R. Vera, M. Bagnara, A. M. Carvajal, W. Aperador, *Int. J. Electrochem. Sci.* 9 (2014) 580.

© 2015 The Authors. Published by ESG ([www.electrochemsci.org](http://www.electrochemsci.org)). This article is an open access article distributed under the terms and conditions of the Creative Commons Attribution license (<http://creativecommons.org/licenses/by/4.0/>).